Istraživanja i projektovanja za privredu
ISSN 1451-4117
DOI:10.5937/jaes0-66040
www.engineeringscience.rs

iipp publishing

Journal of Applied Engineering Science
Original Scientific Paper,
Volume 24, Number 4, Year 2026,
no 1360, pp 648-657

FINITE ELEMENT ANALYSIS OF A COMBINED CULTIVATOR WORKING UNIT WITH REAR ROLLER UNDER LIMIT LOADING

Galin Tihanov[1], Galya Hristova[1]*, Kancho Peychev[1], Yordan Stoyanov[2]

[1]Trakia University, Faculty of Agriculture, Department of Agricultural Engineering, Stara Zagora, Bulgaria
[2]Technical University of Sofia, Plovdiv Branch, Department of Transport and Aircraft Equipment and Technologies, Plovdiv, Bulgaria
**galya.hristova@trakia-uni.bg*

This study presents a structural safety assessment of a combined cultivator working unit comprising cultivator tines and a rear roller using the finite element method (FEM). A three-dimensional model of the structure was developed in the SolidWorks CAD environment and analyzed in SolidWorks Simulation under linear static conditions. Three tine configurations were investigated according to their cross-sectional geometry-circular, square, and rhomboidal-using the same assigned material properties and nominal pressure levels. Soil-tool interaction was simplified by applying a uniformly distributed pressure over the active contact surfaces of the tines and the rear roller. The analysis focused on the highest prescribed pressure of 2.5 kgf/cm² (approximately 0.2452 MPa, reported as 0.25 MPa), adopted as a reference loading scenario for comparative structural assessment. The assessment was carried out using equivalent von Mises stresses, total displacements, and the factor of safety (FOS). The results showed differences in the calculated structural response of the three configurations, including local exceedance of the specified yield criterion for the rhomboidal configuration and the largest resultant displacement for the circular configuration. The analysis evaluated the structural response of the complete assembly, including the cultivator tines, supporting structure, and rear roller. The findings provide a basis for comparing the calculated stresses, displacements, and safety margins of the investigated configurations under the prescribed static loading conditions.

Keywords: finite element analysis, cultivator tine geometry, structural safety, factor of safety, agricultural machinery

HIGHLIGHTS

- Structural response of a combined tine–roller system was assessed under limit loading
- Tine geometry strongly influenced stress distribution and safety margins
- Rhomboidal tines exceeded the yield threshold under the applied load
- Square tines provided the most favorable structural performance

NOMENCLATURE

FEM – finite element method
σvm – equivalent von Mises stress
FOS – factor of safety
URES – total displacement
E – Young's modulus
v – Poisson's ratio
ρ – density
σy – yield strength
σu – ultimate tensile strength

1 Introduction

Tillage is one of the fundamental technological processes in agriculture, significantly influencing the physical properties of soil, its water and air regimes, as well as the conditions for root development and crop yield. Numerous experimental and analytical studies have shown that intensive tillage systems involving multiple machines passes lead to increased soil compaction, rut formation, and degradation of soil structure [1, 2]. It has been established that vertical loading, the number of passes, and machine travel speed are key factors determining the degree of soil compaction and the deterioration of soil agrophysical properties [3].

In response to these negative effects, recent decades have seen the development of technologies aimed at reducing the number of field operations through the use of combined tillage machines. Combined working units enable the execution of multiple operations in a single pass - primary soil cutting and loosening followed by additional crushing and surface leveling. This approach reduces mechanical impact on the soil, lowers energy consumption, and improves the overall quality of soil preparation [4, 5, 6].

However, the efficiency and reliability of such combined systems largely depend on the structural design of the working elements and the interaction between their components. The geometry of cultivator tines, their orientation and mounting configuration, as well as the presence of additional elements such as rear rollers, significantly affect force distribution, stress levels, and deformation patterns within the structure [7, 8]. Therefore, the structural

assessment of combined working units represents an important scientific and practical challenge in agricultural engineering.

Traditional analytical approaches for calculating loads acting on tillage tools are often limited by simplified assumptions related to structural geometry and the complex nature of soil–tool contact interaction. In this context, numerical methods, particularly the finite element method (FEM), have become widely adopted as effective tools for structural and strength assessment of agricultural machinery and their working elements [9, 10, 11], as well as for analyzing soil–tool interaction [12, 13].

In recent years, numerous studies have applied FEM to analyze the interaction between soil and the working elements of agricultural machinery. Hashaam et al. (2023) presented a three-dimensional finite element analysis of cultivator tines and soil deformation, demonstrating a significant influence of tool geometry on stress distribution and draft forces. Similar conclusions were reported by Mahboub & Mardani (2022), who emphasized the role of tine profile in load distribution and structural stability.

In addition to FEM, other numerical approaches such as the discrete element method (DEM) and smoothed particle hydrodynamics (SPH) have been employed, particularly for modeling soil behavior [14, 15]. Nevertheless, FEM remains the preferred method for assessing the structural safety of metallic working elements due to its ability to directly incorporate yield criteria and safety factors, such as the von Mises criterion [16].

A significant limitation of many published studies is that the analyses primarily focus on normal or average operating conditions, under which the structures remain far from their limit states. In practical field conditions, however, tillage machines are frequently subjected to unfavorable and near-limit loading associated with high soil compaction, material heterogeneity, and occasional impact loads. This necessitates so-called worst-case or limit-state analyses, where structural behavior is evaluated in proximity to load-carrying capacity limits [17, 18].

Additional complexity in combined cultivator systems arises from the presence of a rear roller, which actively participates in transferring loads to the frame and influences the distribution of reaction forces. Although rollers are widely used in practice for secondary soil crushing and surface compaction, their role within the overall structural configuration is often not examined in detail in structural analyses. This highlights the need for a systematic approach in which the combined “tine-roller” system is analyzed as an integrated structure.

The present study aims to compare the structural response of three cultivator tine configurations–circular, square, and rhomboidal–within a combined assembly incorporating a rear roller. The assessment uses calculated von Mises stresses, resultant displacements, and factors of safety under prescribed static pressure loading. The rear roller is represented as part of the complete assembly; its individual contribution is not isolated. The study provides a comparative structural assessment within the limitations of the adopted loading, boundary conditions, contact assumptions, and mesh discretization.

2 Materials and methods

2.1 Object of study and geometric modeling

The object of the present study is a combined cultivator working unit consisting of cultivator tines and a rear roller, operating as an integrated structural system. The working unit is designed to perform multiple soil treatment operations within a single pass, including soil loosening, fragmentation, and surface compaction.

A three-dimensional geometric model of the structure was developed in the SolidWorks CAD environment (Fig. 1). The system was modeled as an assembly configuration allowing replacement of the cultivator tines while maintaining identical geometry of the supporting structure and the rear roller. This assembly model was used to evaluate the structural response of the three tine configurations.

The working depth of the cultivator unit was fixed at 12 cm, defining the zone of active interaction between the working surfaces and the soil, and consequently the regions where contact loads were applied. The rear roller was positioned to maintain contact with the soil surface and to actively participate in transferring loads to the machine frame.



Fig. 1. (a) Three-dimensional CAD model of the combined cultivator working unit equipped with cultivator tines and a rear roller



Fig. 1. (b) Three-dimensional CAD model of the combined cultivator working unit equipped with cultivator tines and a rear roller

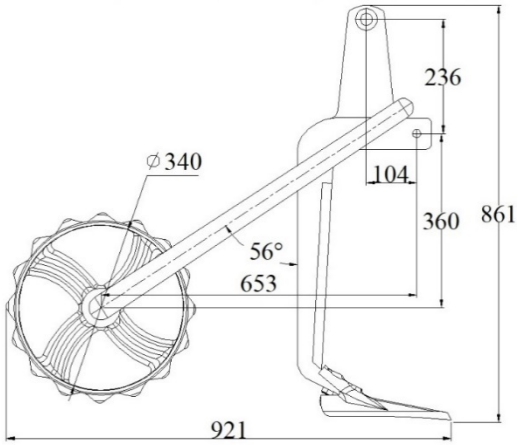

Fig. 1. (c) Three-dimensional CAD model of the combined cultivator working unit equipped with cultivator tines and a rear roller

2.2 Tine configurations

For the purposes of the analysis, three cultivator tine configurations were considered, differing solely in their cross-sectional geometry: circular cross-section, square cross-section, and rhomboidal cross-section.

The configurations were analyzed using the same assigned material properties and nominal pressure levels. However, identical pressure magnitudes do not necessarily produce identical resultant forces when the loaded surfaces differ. The reported mounting selections also differed: three faces were constrained for the square and circular configurations, whereas one edge and two faces were constrained for the rhomboidal configuration. The results therefore compare the complete modeled configurations and do not isolate the influence of cross-sectional geometry alone.

2.3 Material properties

All structural components in the combined model-the supporting structure, cultivator tines, and rear roller-were defined as AISI 4340 steel in the normalized condition, widely used for tillage working elements due to its high strength and good resistance to dynamic loading.

The material was modeled as linear elastic and isotropic, with the following mechanical properties defined in the SI system: Young's modulus E=2.05×1011Pa, Poisson's ratio v=0.32, density ρ=7850 kg.m-³, yield strength σy =7.1×108 Pa, and ultimate tensile strength σu=1.11×109 Pa.

Within the scope of the present study, the material behavior was considered entirely within the elastic regime, enabling the use of the equivalent von Mises stress criterion and the factor of safety as the primary indicators for structural assessment.

2.4 Type of analysis and boundary conditions

The finite element analysis was performed using the SolidWorks Simulation module as a linear static analysis under the assumption of small displacements.

Interactions between the tines, supporting structure, and rear roller were represented using bonded contacts. This assumption prevents relative displacement and separation between the connected surfaces. It does not explicitly represent joint compliance, clearances, frictional slip, or bolt preload in actual bolted or clamped connections.

The boundary conditions were applied by fully constraining the working unit (fixed support condition) of the working unit, corresponding to its attachment to the main machine frame. All translational and rotational degrees of freedom were restricted on the contact surfaces of the mounting brackets.

The distributed pressure was applied to the selected working surfaces using the "Normal To Plane" option, with the Right Plane as the reference. The load was assumed to act over the entire working depth (12 cm) and along the effective contact length of each tine.

The selection of a uniformly distributed pressure is consistent with widely used simplified soil–tool interaction models in FEM-based structural assessments (e.g., Abu-Hamdeh & Reeder, 2003; Hashaam et al., 2023), enabling comparative evaluation under controlled conditions.

2.5 Loading and soil interaction model

The soil action was idealized as a uniformly distributed pressure applied to the selected working surfaces. The maximum prescribed value was 2.5 kgf/cm² (0.2452 MPa), reported approximately as 0.25 MPa. This value was adopted as a reference loading scenario for comparative structural assessment. Published numerical results provide context for its order of magnitude: Karmakar et al. [19] reported a maximum tool-surface pressure of approximately 250 kPa at a tool speed of 1 m/s for a flat tillage tool. However, their result represents a local maximum under different modeling conditions and does not directly validate a uniform pressure over the present

assembly. The adopted value should therefore be interpreted as a prescribed numerical load rather than an experimentally established maximum for a particular soil type.

Gravitational loading was also included in the analysis in order to account for the self-weight of the structure and its influence on the overall structural behavior.

2.6 Finite element mesh and quality verification

A three-dimensional volumetric finite element mesh composed of high-quality tetrahedral elements was used for all model configurations. The mesh was locally refined in regions where elevated stress gradients were expected, primarily in the transition zones between the cultivator tines and the supporting structure, as well as in the contact areas of the rear roller.

For the square and rhomboidal cross-section configurations, approximately 342,000–343,000 nodes and about 211,000 elements were generated. More than 97.6% of the elements exhibited an aspect ratio below 3, while fewer than 0.5% had an aspect ratio greater than 10. For the circular cross-section configuration, approximately 346,000 nodes and 213,000 elements were recorded. These mesh statistics characterize the adopted discretization but do not demonstrate convergence of the peak von Mises stress. A mesh-refinement study under unchanged geometry, loading, contact definitions, and boundary conditions is required to assess the sensitivity of the calculated peak stresses.

2.7 Evaluation criteria

The structural assessment was performed using the following primary indicators:

- Equivalent von Mises stress (σvm);
- Total displacement (URES);
- Factor of safety (FOS), defined as the ratio between the material yield strength and the maximum equivalent stress.

The selected indicators provide a basis for comparing the calculated structural response under the prescribed loading conditions.

3 Results and discussion

3.1 Overall structural response of the combined system under limit loading

At the highest prescribed pressure of 2.5 kgf/cm² (approximately 0.2452 MPa), the three configurations exhibited differences in calculated stresses and displacements. Their structural response was assessed relative to the specified material yield strength under the adopted linear-elastic modeling assumptions.

Regardless of the cross-sectional geometry of the tines, the maximum equivalent von Mises stresses are concentrated in the transition zones between the cultivator tines and the supporting structure, as well as in the regions where the load from the rear roller is transferred into the structure. These stress concentrations reflect the combined effects of the modeled geometry, applied loading, mounting constraints, and contact assumptions.

3.2 Square cross-section – structural performance under limit loading

For the configuration with square cross-section tines (Fig. 2), the maximum recorded equivalent stress reaches σvm, max=5.613×108 Pa, which remains below the yield strength of the selected material. The minimum factor of safety is approximately FOS ≈ 1.265, indicating that the structure remains within the elastic regime even under limit loading conditions.

The stress distribution shows a relatively uniform load transfer along the tine length, with local stress concentrations primarily observed at the edges of the square cross-section and in the transition zone toward the supporting structure. Although square geometry inherently promotes stress concentration at corner regions, under the considered worst-case loading scenario these concentrations do not result in exceeding the yield criterion.

From a structural perspective, the square configuration exhibited the lowest calculated peak stress and the highest minimum factor of safety among the investigated configurations. However, the results suggest the need for careful consideration of transition radii and their potential influence on wear and long-term structural reliability during prolonged operation.

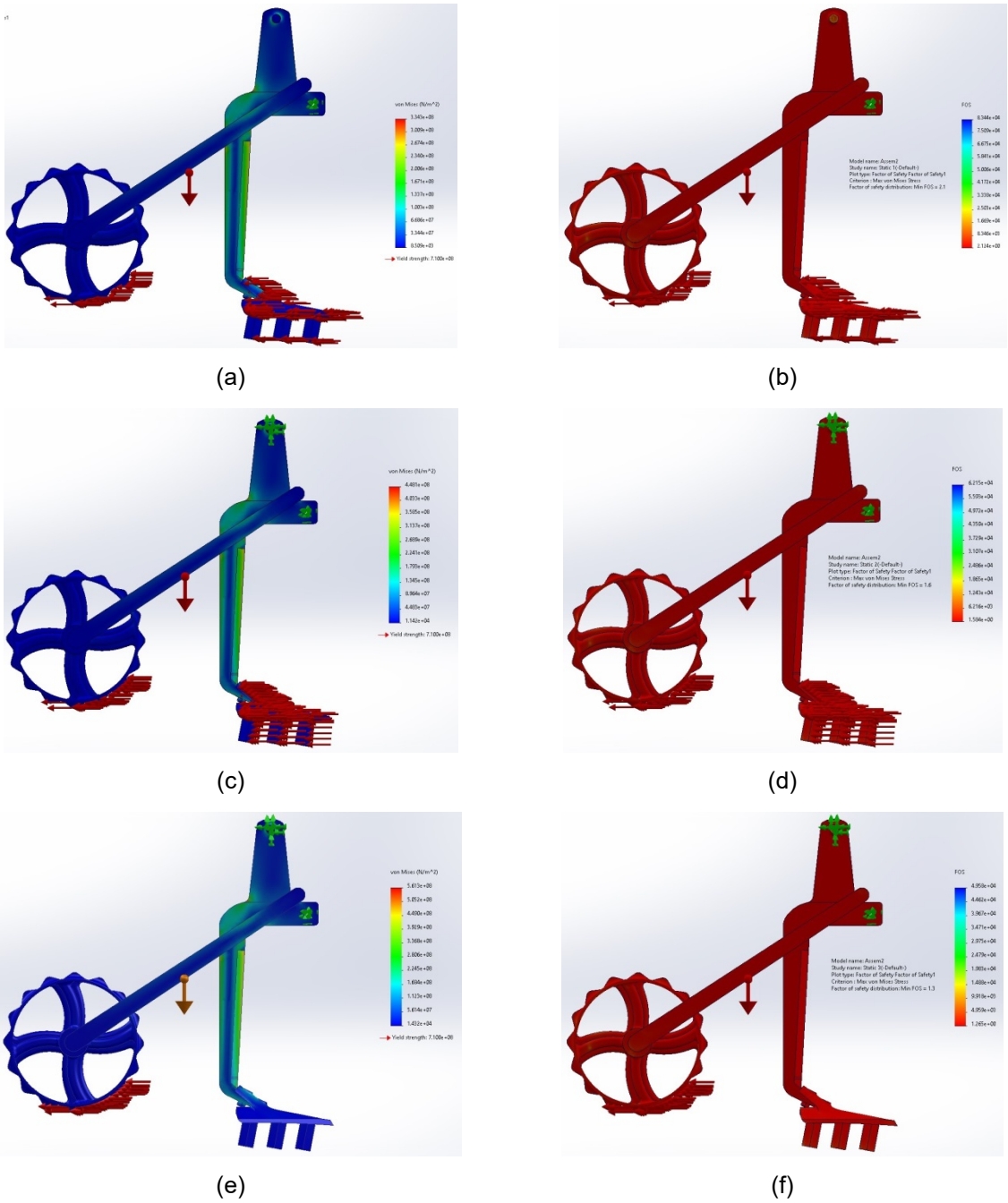

Fig. 2. Distribution of equivalent von Mises stresses and factor of safety (FOS) for the combined working unit with square cultivator tines under contact pressure: (a) 0.15 MPa - σvm, (b) FOS, (c) 0.20 MPa - σvm, (d) FOS, (e) 0.25 MPa - σvm, (f) FOS

3.3 Rhomboidal cross-section – local exceedance of the limit state

For the rhomboidal cross-section configuration (Fig. 3), the maximum calculated von Mises stress was 778 MPa, exceeding the specified material yield strength of 710 MPa. The minimum factor of safety was approximately 0.913. These results indicate local exceedance of the yield criterion in the linear-elastic calculation.

Critical stresses are concentrated in the transition region between the tine and the supporting structure, where the geometry of the rhomboidal profile results in an unfavorable combination of bending and shear effects. It should be emphasized that the observed exceedance of the yield criterion is localized and may be influenced by the adopted “bonded” contact idealization and the simplified soil-tool interaction model. The rhomboidal configuration exhibited the highest calculated peak stress under the prescribed loading conditions.

From an engineering perspective, the findings suggest the need for geometric optimization of the transition zones, modification of fillet radii, or structural adaptation if operation under loading conditions approaching 0.25 MPa is expected (Fig. 3).

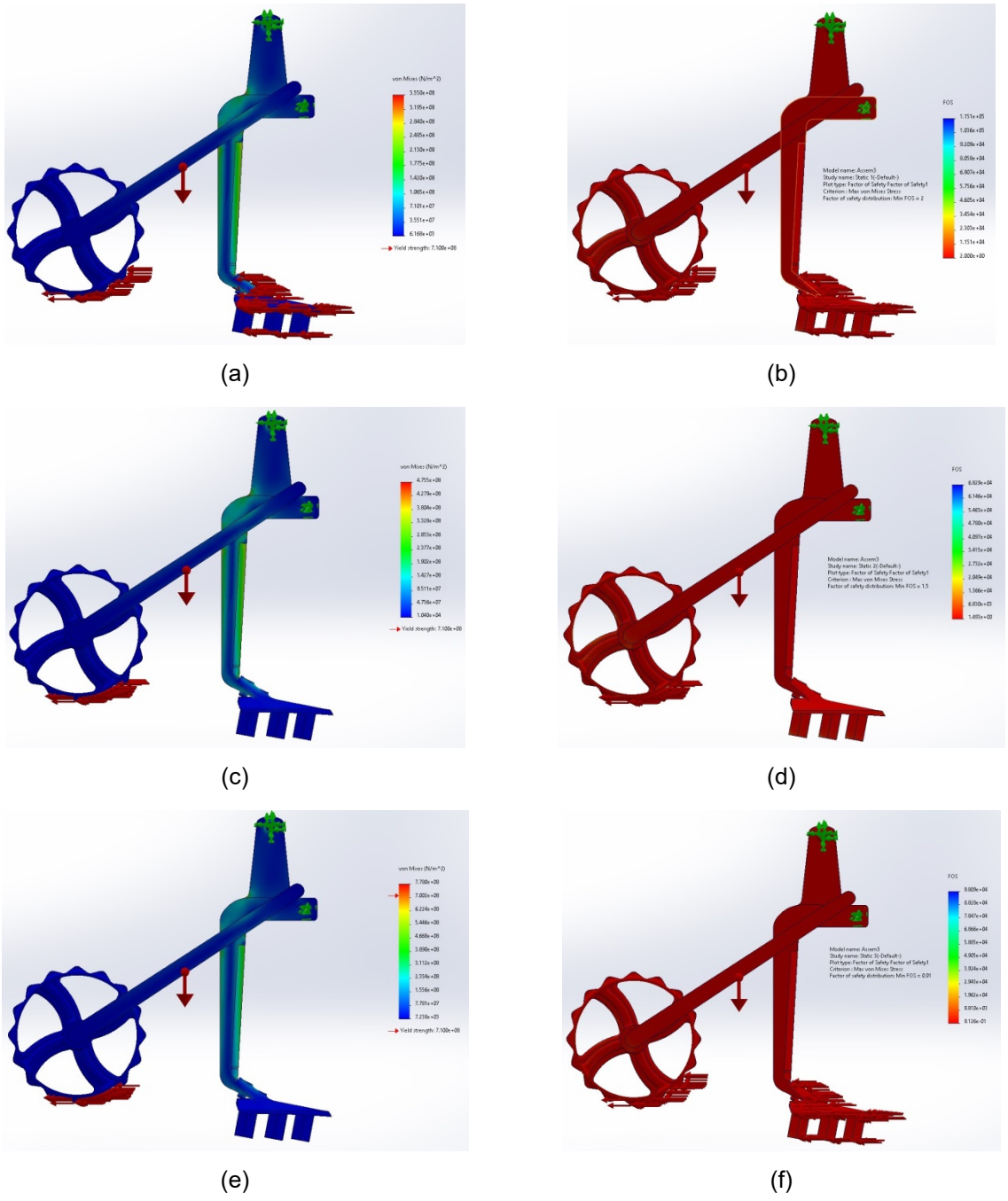

Fig. 3. Distribution of equivalent von Mises stresses and factor of safety (FOS) for the combined working unit with rhomboidal cultivator tines under contact pressure: (a) 0.15 MPa - σ_{vm}, (b) FOS, (c) 0.20 MPa - σ_{vm}, (d) FOS, (e) 0.25 MPa - σ_{vm}, (f) FOS

3.4 Circular cross-section – increased deformations with limited safety margin

For the configuration with a circular cross-section (Fig. 4), the maximum equivalent stress reaches $\sigma vm,max = 6.647\times10^{8}$ Pa, while the minimum factor of safety is approximately FOS ≈ 1.068. This indicates that the structure operates with a very limited safety margin relative to the yield strength.

The maximum calculated resultant displacement was 17.06 mm. This was the largest value among the three investigated configurations under the highest prescribed pressure. No serviceability limit was specified, so this displacement alone does not establish unacceptable operational behavior.

The circular configuration had a smaller calculated margin against yielding than the square configuration. Dynamic response, vibration, and long-term joint reliability were not evaluated in the present static analysis.

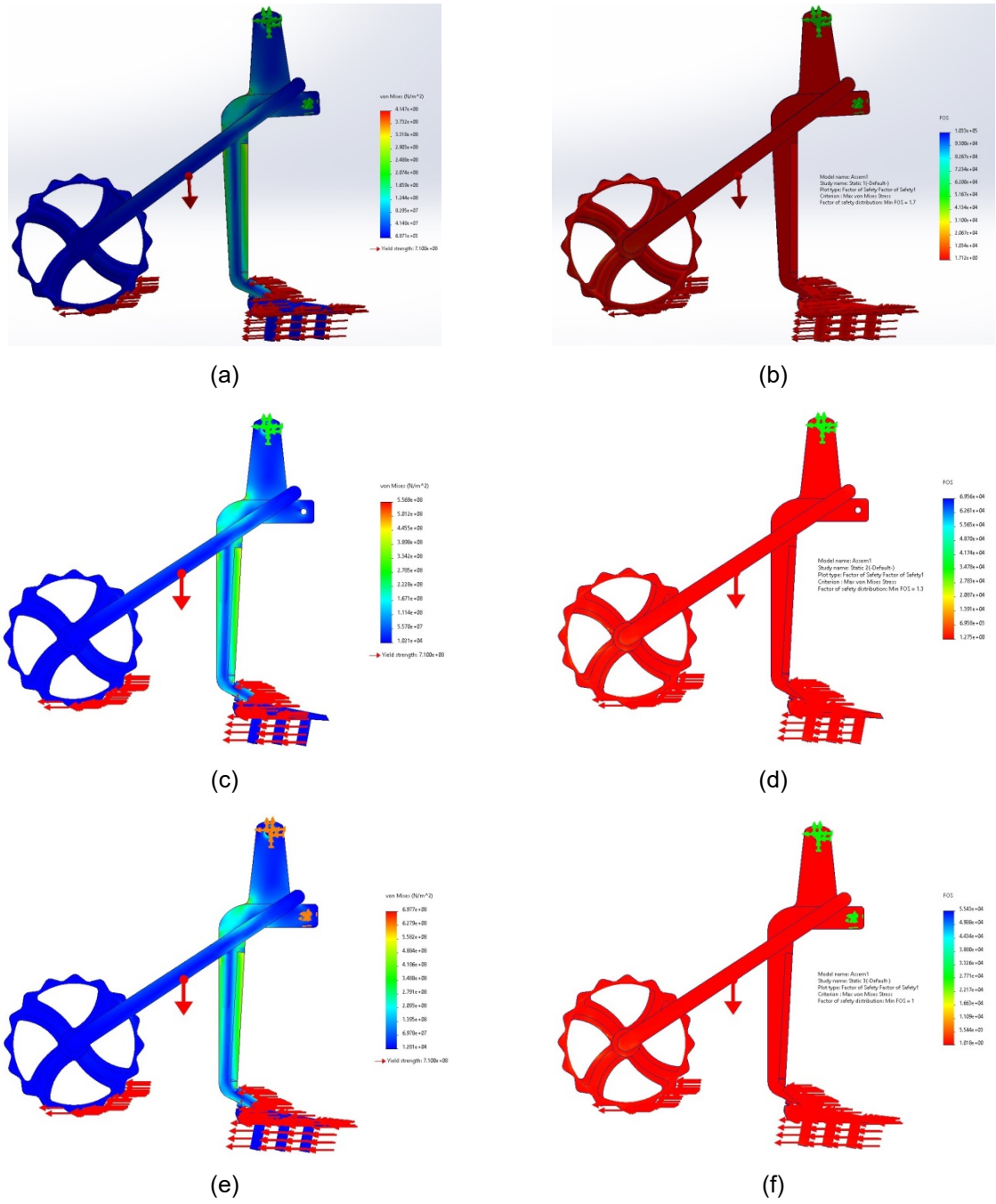

Fig. 4. Distribution of equivalent von Mises stresses and factor of safety (FOS) for the combined working unit with circular cultivator tines under contact pressure: (a) 0.15 MPa - σvm, (b) FOS, (c) 0.20 MPa - σvm, (d) FOS, (e) 0.25 MPa - σvm, (f) FOS

3.5 Overall structural response

Figure 5 compares the calculated maximum von Mises stresses and minimum factors of safety for the three configurations under the highest prescribed pressure. The rhomboidal configuration reached 778 MPa, exceeding the specified yield strength of 710 MPa, whereas the square and circular configurations reached 561.3 MPa and 664.7 MPa, respectively. The exceedance indicates a local violation of the yield criterion in the linear-elastic calculation; it does not establish structural collapse. Similarly, stresses below the yield strength do not independently demonstrate safe field operation.

The minimum factors of safety shown in Figure 5(b) are approximately 1.265 for the square configuration, 1.068 for the circular configuration, and 0.913 for the rhomboidal configuration. These values express the calculated margins relative to the specified yield strength under the adopted modeling assumptions. They do not account for fatigue, impact loading, or plastic redistribution.

Under the prescribed loading and adopted modeling assumptions, the square configuration exhibited the lowest calculated peak stress and the highest minimum factor of safety. The rhomboidal configuration exhibited the highest calculated peak stress and a minimum factor of safety below unity. These findings identify differences between the modeled configurations but do not establish their suitability for field operation.

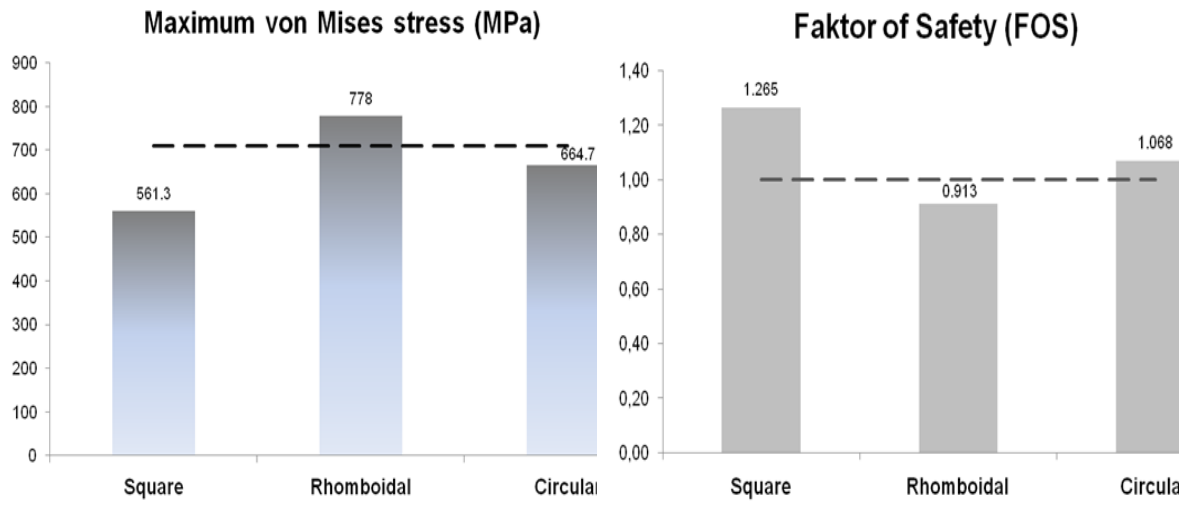

(a) (b)

Fig. 5. Comparative structural performance of different tine geometries under limit loading (0.25 MPa): (a) maximum equivalent von Mises stress; (b) factor of safety (FOS). The dashed lines indicate the material yield strength and the critical safety threshold (FOS = 1), respectively

3.6 Representation of the rear roller

The rear roller was included in the finite element model as part of the combined assembly. The results therefore describe the response of the complete tine–roller system. No reference model without the roller was analyzed. Its individual contribution to load transfer, stiffness, and stress distribution was therefore not quantified.

3.7 Limit-state interpretation

The results allow comparison of the three configurations under the prescribed loading conditions. However, they do not establish a change in their relative ranking between nominal and higher loading levels.

3.8 General discussion

Although experimental validation was not performed within the scope of the present study, the obtained stress patterns and critical regions are consistent with previously reported findings for cantilever-loaded tillage tools [7, 10].

The present finite element model evaluates the structural response under prescribed pressure loading. Comparing the calculated reaction forces with the analytical models of McKyes or Godwin requires soil parameters that were not available for the investigated conditions. Consequently, these models were not used to independently validate the adopted soil loading.

The numerical results describe the structural response of the combined tine–roller assembly under the prescribed loading conditions and show differences in stress levels and displacements between the three tine configurations.

The calculated yield-criterion exceedance for the rhomboidal configuration should be interpreted in the context of the linear-elastic material model, mounting constraints, bonded contacts, and unverified mesh convergence. Further numerical verification is required before attributing the local peak stress to a physical failure mechanism.

The circular configuration exhibited the largest calculated displacement and a minimum factor of safety slightly above unity. These results characterize its response under the prescribed static loading but do not establish fatigue life, vibration behavior, or long-term operational reliability.

Including the rear roller allows the combined assembly to be assessed. However, a comparison with a model without the roller is needed to determine its individual influence on the structural response.

The results provide a comparative assessment of the modeled configurations under prescribed static loading.

It should be noted that the adopted soil interaction model represents a simplified idealization that does not account for local heterogeneity, dynamic effects, or nonlinear soil behavior. Non-uniform soil resistance may change both the magnitude and position of the resultant force on each tine. This can alter bending moments and local stress concentrations. Even at the same resultant force, a load acting farther from the mounting region produces a larger bending moment. Uniform pressure does not capture these variations and may therefore underestimate or overestimate local stresses. Nevertheless, this approach is widely used in preliminary structural assessments and is suitable for identifying critical zones and for comparative evaluation of structural safety under limit loading. Future research may extend the analysis by incorporating nonlinear material models, advanced contact interactions, and dynamic loading conditions in order to achieve a more comprehensive assessment of operational reliability.

The bonded contact assumption may overestimate assembly stiffness compared with connections that allow local deformation or slip. It may also alter load transfer and local stress concentrations near the mounting interfaces. The magnitude and direction of these effects were not quantified in the present study. Stresses in these regions should

therefore be interpreted with caution. A more detailed representation of the actual connections would be needed to assess their influence.

4 Conclusions

The finite element analysis compared three tine configurations within a combined cultivator tine–roller assembly under prescribed static loading. The highest applied pressure was 2.5 kgf/cm² (approximately 0.2452 MPa, reported as 0.25 MPa), adopted as a reference loading scenario rather than an experimentally established maximum soil pressure.

The square configuration exhibited the lowest calculated maximum von Mises stress of 561.3 MPa and the highest minimum factor of safety of approximately 1.265 among the investigated configurations.

The rhomboidal configuration exhibited a maximum calculated von Mises stress of 778 MPa and a minimum factor of safety of approximately 0.913, indicating local exceedance of the specified yield criterion in the linear-elastic calculation.

The circular configuration exhibited a maximum calculated von Mises stress of 664.7 MPa, a minimum factor of safety of approximately 1.068, and the largest reported resultant displacement of 17.06 mm.

The rear roller was included in the combined structural model. Its individual influence was not quantified because no reference model without the roller was analyzed.

These findings describe the investigated configurations under the adopted loading, boundary conditions, contact assumptions, and mesh discretization. They do not independently establish field safety, fatigue life, or long-term operational reliability. Mesh-convergence verification and independent validation remain necessary.

5 Acknowledgments

This research was carried out within the framework of research project 1AF/25 entitled *"Influence of Cultivator Working Unit Parameters and Their Impact on Soil"*, funded by Trakia University – Stara Zagora.

6 References

[1] Pulido-Moncada, M., Munkholm, L. J., & Schjønning, P. (2019). Wheel load, repeated wheeling, and traction effects on subsoil compaction in northern Europe. *Soil and Tillage Research, 186*, 300–309. https://doi.org/10.1016/j.still.2018.11.005

[2] Oliveira, E. M., Wittwer, R., Hartmann, M., Keller, T., Buchmann, N., & Van der Heijden, M. G. A. (2024). Effects of conventional, organic and conservation agriculture on soil physical properties, root growth and microbial habitats in a long-term field experiment. *Geoderma, 447*, Article 116927. https://doi.org/10.1016/j.geoderma.2024.116927

[3] Farhadi, N., Mardani, A., Hosainpour, A., Golanbari, B., & Nazari Chamki, A. (2025). Impact of vertical load, multiple passes, and speed on rut depth in soil under pneumatic and track wheels. *Scientific Reports, 15*, Article 27890. https://doi.org/10.1038/s41598-025-13535-w

[4] Manushkov, S., Mitev, G., & Demirev, Zh. (2013). Machines for soil tillage without mouldboard ploughing. *Scientific Works of the University of Ruse, 52(1.1),* 191–197.

[5] Prem, M., Swarnkar, R., Kantilal, V. D. K., Jeetsinh, P. S. K., & Chitharbhai, K. B. (2016). Combined tillage tools—A review. *Current Agriculture Research Journal, 4(2)*, 179. https://doi.org/10.12944/CARJ.4.2.07

[6] Behera, A., Raheman, H., & Thomas, E. V. (2021). A comparative study on tillage performance of rota-cultivator (a passive–active combination tillage implement) with rotavator (an active tillage implement). *Soil and Tillage Research, 207,* Article 104861. https://doi.org/10.1016/j.still.2020.104861

[7] Tekeste, M. Z., Balvanz, L. R., Hatfield, J. L., & Ghorbani, S. (2019). Discrete element modeling of cultivator sweep-to-soil interaction: Worn and hardened edges effects on soil–tool forces and soil flow. *Journal of Terramechanics, 82,* 1–11. https://doi.org/10.1016/j.jterra.2018.11.001

[8] Lejman, K. (2018). Vertical forces acting on cultivator tines in the aspect of shearing speed and flexibility of tines. *Agricultural Engineering, 22(1)*, 39–48. https://doi.org/10.1515/agriceng-2018-0014

[9] Yang, J. (2024). Strength calculation method of agricultural machinery structure using finite element analysis. *International Journal of Advanced Computer Science and Applications, 15(10)*, 699–706. https://doi.org/10.14569/IJACSA.2024.0151071

[10] Mahboub Yangeje, H., & Mardani, A. (2022). Investigating the interaction between soil and cultivator blade by numerical simulation and validation of results by soil bin tests. *Journal of Agricultural Machinery, 12(4),* 587–599. https://doi.org/10.22067/jam.2021.70572.1041

[11] Velloso, N. S., Costa, A. L., Magalhães, R. R., Santos, F. L., & Andrade, E. T. (2018). The finite element method applied to agricultural engineering: A review. *Current Agriculture Research Journal, 6(3),* 286–299. https://doi.org/10.12944/CARJ.6.3.08

[12] Abu-Hamdeh, N. H., & Reeder, R. C. (2003). Nonlinear 3D finite element analysis of the soil forces acting on a disk plow. *Soil and Tillage Research, 74(2)*, 115–124. https://doi.org/10.1016/S0167-1987(03)00152-1

[13] Hashaam, M., Waqar Akram, M., Ahmad, M., Akram, M. Z., Faheem, M., Maqsood, M., & Aleem, M. (2023). 3D finite element analysis of tine cultivator and soil deformation. *Research in Agricultural Engineering, 69(3)*, 107–117. https://doi.org/10.17221/58/2022-RAE

[14] Shmulevich, I. (2010). State of the art modeling of soil–tillage interaction using discrete element method. *Soil and Tillage Research, 111(1)*, 41–53. https://doi.org/10.1016/j.still.2010.08.003

[15] Hu, M., Gao, T., Dong, X., Tan, Q., Yi, C., Wu, F., & Bao, A. (2023). Simulation of soil–tool interaction using smoothed particle hydrodynamics (SPH). *Soil and Tillage Research, 229,* Article 105671. https://doi.org/10.1016/j.still.2023.105671

[16] SolidWorks Corporation. (2022). Failure criteria. SOLIDWORKS Design Help. https://help.solidworks.com/2022/English/SolidWorks/cworks/Failure_Criteria.htm

[17] Ibrahimi, A., & Bentaher, H. (2025). Simulation of tillage forces and soil movement during soil–disc plow interaction using FEM. *Scientific Reports, 15,* Article 36022. https://doi.org/10.1038/s41598-025-19961-0

[18] Song, W., Ren, L., Wang, J., Ma, Y., Guo, Y., Han, M., & Zhao, H. (2025). Methods for constructing soil dynamic models under intelligent cultivation: Dynamic interaction mechanisms between farming tools with complex structures and soil. *Agriculture, 15(13)*, Article 1355. https://doi.org/10.3390/agriculture15131355

[19] Karmakar, S., Kushwaha, R. L., & Laguë, C. (2007). Numerical modelling of soil stress and pressure distribution on a flat tillage tool using computational fluid dynamics. *Biosystems Engineering, 97(3)*, 407–414. https://doi.org/10.1016/j.biosystemseng.2007.02.008

7 Conflict of interest statement

The authors declare no conflict of interest.

8 Author contributions

Galin Tihanov: review and editing. Galya Hristova: conceptualization, methodology, formal analysis, writing of the original draft. Kancho Peychev: review and editing. Yordan Stoyanov: conceptualization, methodology, formal analysis.

9 Data availability statement

The data supporting the findings of this study are available from the corresponding author upon reasonable request.

10 Supplementary materials

No supplementary materials are available.

Paper submitted: 25.03.2026.
Paper accepted: 22.10.2026.
This is an open access article distributed under the CC BY 4.0 terms and conditions